

Holographic Instanton Liquid and chiral transition

Bogeun Gwak^{a,b}, Minkyoo Kim^{a,b}, Bum-Hoon Lee^{a,b}, Yunseok Seo^b and Sang-Jin Sin^c

^a*Department of Physics, Sogang University, Seoul 121-742, Korea*

^b*Center for Quantum Spacetime, Sogang University, Seoul 121-742, Korea*

^c*Department of Physics, Hanyang University, Seoul 133-791, Korea*

Email: rasenis@sogang.ac.kr, mkim80@sogang.ac.kr, bhl@sogang.ac.kr, yseo@sogang.ac.kr, sjs@hanyang.ac.kr

ABSTRACT: We study the phase diagram of *black* D3 geometry with uniformly distributed D-instanton charge using the probe D7 brane. In the presence of uniform D-instanton charges, quarks can be confined although gluons are not, because baryon vertices are allowed due to the net repulsive force on the on the probe D-branes. Since there is no scale in the geometry itself apart from the horizon size, there is no Hawking-Page transition. As a consequence, the D7 brane embedding can encode the effect of the the finite temperature as well as finite baryon density even for low temperature. The probe D-brane embedding, however, undergoes a chiral phase transition according to the temperature and density parameter. We studied such phase transitions and calculated the constituent quark mass, chiral condensation and the binding energy of baryons as function of the density. The baryon vertex melting is identified as the quark deconfinement. We draw phase diagram according to these transitions.

KEYWORDS: Gauge/gravity duality, instanton, chiral symmetry.

Contents

1. Introduction	1
2. Background geometry and D-brane setup	4
3. Chiral condensation at zero density	5
3.1 Zero temperature limit	5
3.2 Finite temperature without density	7
4. Chiral symmetry at Finite temperature and finite baryon density	10
4.1 Quark phase	11
4.2 Baryon phase	13
5. Phase Transition	15
5.1 Canonical ensemble	16
5.2 Relation between chemical potential and density	19
5.3 Grand canonical ensemble	21
5.4 Chiral condensation	22
6. Summary and Discussion	23
A. Chern-Simons term	25
B. Hamiltonian density of baryon vertex	27
C. Force balance condition	29

1. Introduction

One of the difficulty in holographic QCD is to discuss the temperature dependence of physical observables in the hadron phase. The problem is the presence of the Hawking-Page transition as the deconfinement/confinement transition [1]: background metric describing the low temperature phase does not contain any temperature parameter. Describing the hadrons in finite temperature requests having a black hole metric, in which gluons are always deconfined. Therefore we are lead to the question whether quark can be confined while gluons are deconfined. In fact the degree of freedom of two species are different in large N_c order and the confinement of gluons and that of quarks should be separate phenomena at least in large N_c limit. However, in most of the geometric background with

well defined Hawking temperature, a baryon vertex [2] is not allowed as a finite energy solution[3, 4], because black D-brane has net attractive gravity.

To have a phase transition, we need a scale other than the temperature. In QCD, scale invariance is broken by the chiral and gluon condensation, and it is also known that both of them are induced by the presence of the instanton. There has been huge activity to utilize the instanton background in gauge theory and (quark) dynamics in the instanton background has been practiced by many the topic directly relevant to our paper is the instanton gas/liquid model, where mass generation and the chiral symmetry breaking was discussed using the anomaly and fermion zero modes. For a review, see the review article by Schafer and Shuryak [5] and references therein.

It is also well known that the D-instanton is the gravity dual to the Yang-Mill instanton. Therefore, it is very natural to try to use a background dual to the instanton gas. In fact, a background which is dual to the uniformly distributed D-instanton over D3 was suggested by Hong Liu and Tseytlin [6], where they also proposed, naturally, that the D3/D-instanton geometry is dual of the N=4 Yang Mill theory with constant gluon condensation with zero electric/magnetic gluon field, that is $\langle F_{\mu\nu} \rangle = 0$, $\langle \text{Tr} F^{\mu\nu} F_{\mu\nu} \rangle = cq \neq 0$ where F is field strength of the gauge fields. Such D3/D-instanton geometry contains non-trivial dilaton giving non-zero value of gluon condensation q , which was identified precisely as the D-instanton density.

While the chiral symmetry breaking was a natural consequence of the instanton background, the confinement, was not directly reachable in the gauge theory instanton gas model. One of the interesting consequence of the AdS/CFT is that Liu and Tseytlin actually have shown that the background has a confinement with a linear quark-antiquark potential. Therefore in the gravity dual, both the chiral condensation and confinement turns out to be consequences of the presence of the D-instanton charges, which produce effectively net repulsive force on the probe D-branes and the probe Fundamental strings.

The purpose of this paper is to consider the finite temperature and density of the holographic dual of the D instanton gas/liquid. For our purpose, we need to extend the geometry of Liu and Tseytlin to the finite temperature. The necessary metric was found by Ghoroku et al. [9] in the context completely unrelated to instanton gas model. While most of the dilaton gravity solution is singular [7, 8] such that temperature is ill-defined, their solution allows a Hawking temperature. The geometry is quasi-confining, namely, it has following properties [9]: (i) gluons are deconfined: In QCD, one can consider the gluon propagator directly and state the (de)confinement. However, in hQCD, one can not look at the gluon propagator directly since that is colored object whose treatment is beyond the gravity limit. Instead, what one looks at is the spectrum of the dilaton field which is dual of the glueball operator. IF that spectrum is well peaked or discrete, this is the signal of confinement. If the spectral function does not show any peak or feature, it means they are all dis-integrated and gluons are in de-confined state. As a theorem, the presence of the horizon does not allow any stable glueball spectrum, because in AdS black hole, quasi-normal mode spectrum has large imaginary part. (ii) the quark-anti quark potential is Coulomb like for short distance, linear for medium distance and screened for large enough distances. The turn-over distance depends on temperature and gluon condensation. (iii)

Baryon vertex solution is allowed in low enough temperature.

There is no geometric transition as temperature grows because (i) we do not have any compactified direction, (ii) We need to work out the thermodynamics of the bulk theory in Einstein frame, in which our geometry is the same as the black D3 brane, (iii) the action for the dilaton and axion cancel each other. The difference between the black D3 brane with and without D-instantons comes from the probe D-brane dynamics, which should be calculated in the string frame where dilaton factor is manifest as an over all factor in the metric. It turns out that the Chern-Simons term can not cancel the effect of the dilaton unlike the claim of reference [9], which is the origin of the chiral symmetry breaking in our paper. On the other hand, in [9], the flat embedding is preferred for some reason and it was attributed to the cancellation of the dilaton effect by the CS term. As we have shown in the appendix A, this is not the case and brane embedding can not be flat, which in turn induces the chiral symmetry breaking. We attribute such effect to the net repulsive force acting on probe D7 created by the D-instanton charges. Such breaking of the chiral symmetry is consistent with the gauge theory where zero mode of the fermions in the D-instanton background requests chiral symmetry breaking.

For the treatment of chemical potential, we follow the method first suggested in [12, 13] and developed in [14, 15]. There are two types of probe brane embedding: one describes quark phase, where the flavor brane touches the black hole horizon and a baryon vertex is not allowed. Usually this embedding is called *black hole embedding*. If there are strings connecting the horizon and the D7, the latter is deformed to a spiky brane to touch the horizon. The other embedding is the one where D7 brane never touches the horizon. On such brane, strings can be attached only if a baryon vertex (BV) is allowed and present so that the strings connect the BV to D7. We find that there is a phase transition between two embeddings. We also find that there is a transition between the two black hole embeddings. The binding energy of the baryon and the melting temperature in this background was studied in [10, 11] by considering one baryon vertex connected to the boundary at infinity by N_c strings. We treat the baryonic medium using the method developed in [4] where each compact baryon vertex is joined with a D7 probe brane through a funnel and such configuration is smeared along the D3 direction.

One final comment here is about the nomenclature: usually instanton gas is for weakly interacting far-separated instanton and liquid is for dense and non-trivial interaction. Here we are using the words "instanton liquid" since homogenous distribution would not be consistent with the well separated gas configuration. We do not focus on the interaction strength at all.

The rest of the paper is planned as follows. In section 2, the background geometry is reviewed and various embedding configuration was studied with zero density and chiral condensations are calculated. In section 3, we study how the embedding geometry changes as we vary 3 parameters: temperature, baryon/quark density and the gluon condensation. We find that there can be two phases within quark phase: one chiral symmetry broken and the other chiral symmetry restored. In section 4, by calculating the free energy and chemical potential as function of density we study the phase transition between the baryon and quark phases as well as the phase transition between the two quark phases. We work

out the complete phase diagram both in canonical and grand canonical ensemble. In section 6, we give a conclusion and future directions. In the appendix show that the Chern-Simons term can not cancel the effect of the dilaton unlike the reference [9].

2. Background geometry and D-brane setup

Here we will briefly review the background geometry and the probe brane setup within it. The geometry is the one that is a finite temperature extension of D3/D-instanton background with Euclidean signature given by [9]. The background has a five-form field strength and a axion field which couples to D3 and D-instanton, respectively. The ten dimensional supergravity action in Einstein frame is given by [16, 17]

$$S = \frac{1}{\kappa} \int d^{10}x \sqrt{g} \left(R - \frac{1}{2} (\partial\Phi)^2 + \frac{1}{2} e^{2\Phi} (\partial\chi)^2 - \frac{1}{6} F_{(5)}^2 \right), \quad (2.1)$$

where Φ and χ denote the dilaton and the axion respectively. If we set $\chi = -e^{-\Phi} + \chi_0$, the dilaton term cancel the axion term in (2.1). Then the action becomes that of the metric and five-form. The solution in string frame can be written as

$$\begin{aligned} ds_{10}^2 &= e^{\Phi/2} \left[\frac{r^2}{R^2} (f(r)^2 dt^2 + d\vec{x}^2) + \frac{1}{f(r)^2} \frac{R^2}{r^2} dr^2 + R^3 d\Omega_5^2 \right], \\ e^{\Phi} &= 1 + \frac{q}{r_T^4} \log \frac{1}{f(r)^2}, \quad \chi = -e^{-\Phi} + \chi_0, \\ f(r) &= \sqrt{1 - \left(\frac{r_T}{r}\right)^4}, \end{aligned} \quad (2.2)$$

where $R^4 = 4\pi g_s N_c \alpha'^2$. The constant q denotes the number of D-instanton. From the AdS/CFT dictionary, it also represents the vacuum expectation value (vev) of gluon condensation. The dilaton factor diverges at the black hole horizon. However, it does not give any effect on the thermodynamics of the *bulk theory* since the latter should be calculated in the Einstein frame where its onshell action is the same as that of the black D3 brane solution. The geometry has a regular event horizon and Hawking temperature given by $T = r_T/\pi R^2$.

Quark-antiquark potential is derived from the expectation value of a Wilson loop using U-shaped fundamental string configuration [9]. For a given temperature T , U-shaped string touches the black hole horizon and splits into two straight strings at certain separation $L_*(T)$. This critical distance L_* increases as temperature decreases as in the usual black hole geometry. The geometry corresponds to deconfined phase from the gluon point of view. In usual black D3 brane geometry, $q\bar{q}$ potential is Coulomb like for small separation and flat when separation is larger than L_* , where it is completely screened. In this background, the potential is Coulomb like at short distances but linearly grows until U-shaped string touches the horizon. At zero temperature the potential is linear up to indefinitely large distance. This is a similarity to the real QCD. But the gluon is deconfined which is different from the real QCD. We call such phenomena as ‘quasi-confinement’. Such quasi-confining property comes from the presence of q , which is the value of gluon condensation. It is the

D-instanton number and it should be closely related to the chiral condensation as well as the gluon condensation.

Introducing a dimensionless coordinate ξ by $\frac{d\xi^2}{\xi^2} = \frac{dr^2}{r^2 f^2(r)}$, the background geometry can be rewritten as

$$ds^2 = e^{\Phi/2} \left[\frac{r^2}{R^2} (f(r)^2 dt^2 + d\vec{x}^2) + \frac{R^2}{\xi^2} (d\xi^2 + \xi^2 d\Omega_5^2) \right], \quad (2.3)$$

where r and ξ are related by

$$\left(\frac{r}{r_T} \right)^2 = \frac{1}{2} \left(\frac{\xi^2}{\xi_T^2} + \frac{\xi_T^2}{\xi^2} \right), \quad \text{and} \quad f = \left(\frac{1 - \xi_T^4/\xi^4}{1 + \xi_T^4/\xi^4} \right) \equiv \frac{\omega_-}{\omega_+}, \quad \omega_{\pm} \equiv 1 \pm \frac{\xi_T^4}{\xi^4}. \quad (2.4)$$

To describe the embedding of the probe D7 brane, we decompose \mathbb{R}^6 part in (2.3) into $\mathbb{R}^4 \times \mathbb{R}^2$,

$$ds^2 = e^{\Phi/2} \left[\frac{r^2}{R^2} (f(r)^2 dt^2 + d\vec{x}^2) + \frac{R^2}{\xi^2} (d\rho^2 + \rho^2 \Omega_3^2 + dy^2 + y^2 d\phi^2) \right]. \quad (2.5)$$

D7 brane spans (t, \vec{x}, ρ) direction and wraps S^3 , and is perpendicular to y and ϕ direction. We can set $\phi = 0$ using the $SO(2)$ symmetry in x^8, x^9 plane. Then induced metric on D7 brane becomes

$$ds_{D7}^2 = e^{\Phi/2} \left[\frac{r^2}{R^2} (f(r)^2 dt^2 + d\vec{x}^2) + \frac{R^2}{\xi^2} ((1 + y'^2) d\rho^2 + \rho^2 \Omega_3^2) \right], \quad (2.6)$$

where y' denotes to $\partial y(\rho)/\partial \rho$ and $\xi^2 = \rho^2 + y^2$.

The general action of probe D7 brane can be written as sum of DBI action of D7 brane and the Chern-Simons term. The embedding dynamics of the D7 brane gives the dependence of the chiral condensation on control parameters like temperature, density, quark mass etc. as we will describe below.

3. Chiral condensation at zero density

Here we study D7 brane embeddings at zero density but we first consider the zero temperature and zero density case to study q dependence of the chiral condensation and then consider the finite temperature to study chiral phase transition temperature as a function of gluon condensation.

3.1 Zero temperature limit

In this limit, 10 dimensional geometry (2.2) becomes near horizon geometry of D3/D-instanton system which preserve half of supersymmetry [6],

$$ds^2 = e^{\Phi/2} \left[\frac{r^2}{R^2} (dt^2 + d\vec{x}^2) + \frac{R^2}{r^2} (dr^2 + r^2 d\Omega_5^2) \right],$$

$$e^{\Phi} = 1 + \frac{q}{r^4}, \quad \chi = -e^{-\Phi} + \xi_{\infty}. \quad (3.1)$$

Induced metric on D7 brane can be written as

$$ds_{D7}^2 = e^{\Phi/2} \left[\frac{r^2}{R^2} (dt^2 + d\vec{x}^2) + \frac{R^2}{r^2} ((1 + y'^2)d\rho^2 + \rho^2 d\Omega_3^2) \right], \quad (3.2)$$

where $r^2 = \rho^2 + y^2$. The presence of D-instanton implies that of axion. The axion can couple to the D7 brane world volume through the Chern-Simons term. Therefore D7 brane action can be written as

$$\begin{aligned} S_{D7} &= S_{DBI} + S_{CS} \\ &= -\mu_7 \int d\sigma^8 e^{-\Phi} \sqrt{-\det(g + 2\pi\alpha' F)} + \mu_7 \int d^8\sigma \frac{1}{8!} C_{(8)i_1 \dots i_8}, \end{aligned} \quad (3.3)$$

where σ is world volume coordinates of D7 brane, g is induced metric on D7 brane and $C_{(8)}$ is the Hodge dual 8-form gauge potential of axion field which is 0 form. If we fix D7 brane position along the fixed ϕ direction, the Chern-Simons term becomes locally total derivative as we proved in appendix A. Therefore it can not affect the equation of motion hence we can ignore the Chern-Simons term. This observation makes the key difference of our D7 brane embedding to the one described in [9] and it will be the origin of the chiral symmetry breaking.

Now, the DBI action for D7 brane can be written as

$$S_{D7} = -\tau_7 \int dt d\rho e^{\Phi} \rho^3 \sqrt{1 + y'^2}, \quad (3.4)$$

with $\tau_7 = \mu_7 V_3 \Omega_3$ and the equation of motion is

$$\frac{d}{d\rho} \left(\frac{e^{\Phi} \rho^2 y'}{\sqrt{1 + y'^2}} \right) + \frac{q \cdot y \rho^3 e^{\Phi} \sqrt{1 + y'^2}}{r^6} = 0. \quad (3.5)$$

For a generic value of q , analytic solution is not available. So we look for numerical one. For $q = 0$, the trivial embedding $y = \text{constant}$ is a solution which is consistent with the result in [19].

If we turn on q , the solution deforms. The bare quark mass m_q and chiral condensation c are encoded in the asymptotic form of embedding function $y(\rho)$ [20, 21]:

$$y(\rho) = m_q + \frac{c}{\rho^2} + \dots \quad (3.6)$$

The embeddings with fixed m_q are drawn in Figure 1. As q increases, probe D7 brane in the central region bends upward more and more so that we have non-vanishing chiral condensation that is an increasing function of q . The value q corresponds to the gluon condensation $\langle \text{Tr} F^2 \rangle$ in boundary theory and hence plays the role of parameter of scale symmetry breaking. The m_q dependence of chiral condensation is drawn in Figure 2(a). With non-zero value of q , the value of chiral condensation goes to finite value in ($m_q \rightarrow 0$). Therefore, the chiral symmetry is broken. The q dependences of the chiral condensation for given m_q are drawn in Figure 2(b). The condensation is increasing function of q but

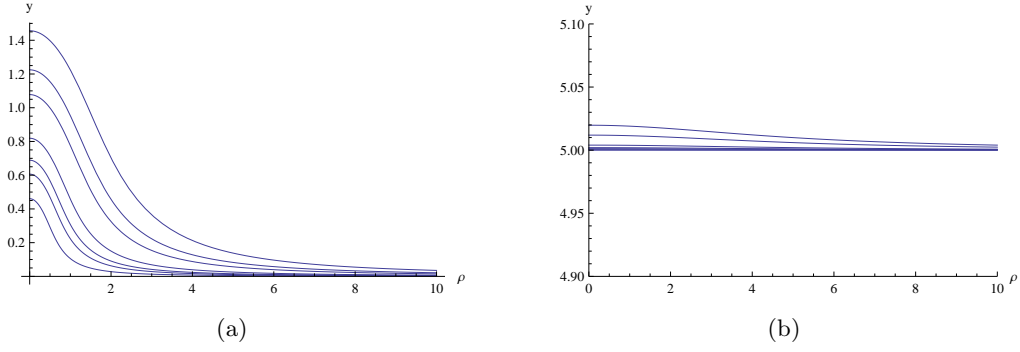


Figure 1: (a) D7 brane embeddings for $m_q = 0$ with $q = 0, 0.1, 0.3, 0.5, 1, 3, 5, 10$ from bottom to top. (b) D7 brane embeddings for $m_q = 5$ with $q = 0, 0.1, 0.3, 0.5, 1, 3, 5, 10$ from bottom to top .

decreasing one of m_q . At large quark mass, chiral condensation is linearly in q . It is consistent with the expectation from field theory [23, 21, 22],

$$\langle \bar{\psi}\psi \rangle = \frac{\alpha_s N_f}{12\pi m_q} \langle \text{Tr} F^2 \rangle . \quad (3.7)$$

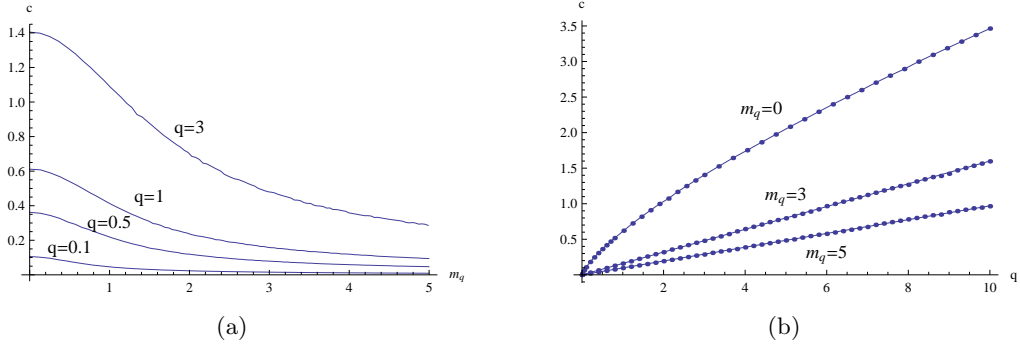


Figure 2: (a) m_q dependence of chiral condensation with fixed q . (b) q dependence of chiral condensation with fixed m_q .

3.2 Finite temperature without density

In this section, we will study D7 brane embedding in black hole geometry without chemical potential. We use the black hole metric (2.2) and induce metric on D7 brane with (2.6). Then DBI action for D7 brane becomes

$$S_{D7} \equiv \tau_7 \int dt d\rho V(\rho, y) \sqrt{1 + y'^2}, \quad (3.8)$$

where $\tau_7 = \xi_T^4 \mu_7 V_3 \Omega_3$ and $V = e^\Phi \rho^3 \omega_+ \cdot \omega_-$. The dilaton factor seems to diverge at the black hole horizon. However, the dilaton factor e^Φ comes with ω_- which contains the zero

$\sim (r - r_T)$ at the horizon. This zero is enough to kill the logarithmic divergence of the dilaton. In other words, the dilaton's log singularity does not change the qualitative behavior of the brane dynamics near the horizon.

The equation of motion for the DBI action can be written following form

$$\frac{y''}{1+y'^2} + \frac{\partial \log V}{\partial \rho} y' - \frac{\partial \log V}{\partial y} = 0. \quad (3.9)$$

This equation of motion is highly non-linear. We can get solution only in numerical way with proper boundary condition (BC). In the presence of black hole horizon, embedding of probe D7 can be classified as 'Minkowski embedding' and 'black hole embedding' [24]. For the Minkowski embedding, we impose BC: $y(0) = y_0$ and $y'(0) = 0$. For the black hole embedding, BC is determined by regularity condition of equation of motion at the horizon:

$$y(\rho_{min}) = y_0, \quad y'(\rho_{min}) = \tan \theta, \quad (3.10)$$

where θ is the angle between ρ axis and probe brane position at the horizon. In usual black hole geometry, gravitational attraction of black hole bends the probe brane downward. However, non-zero value of q gives net 'repulsive' force on probe D7. Therefore, D7 bends upward. q dependences of Minkowski embedding and black hole embedding are drawn in Figure 3. For fixed quark mass and temperature, the bigger is q , the more pushed up is the D7 brane. Such effect is common both in Minkowski and black hole embedding.

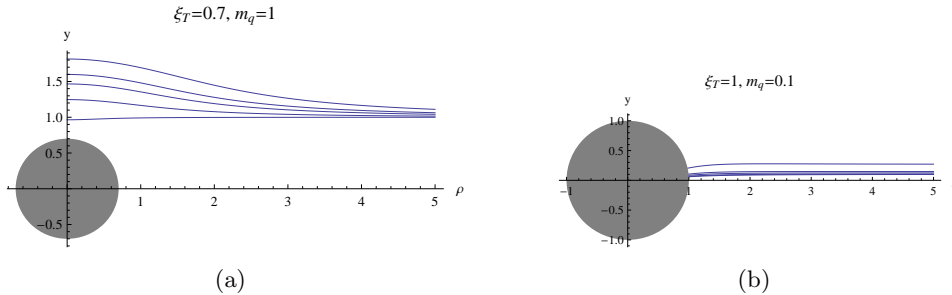


Figure 3: (a) q dependence of Minkowski embedding for $m_q = 1$ with $q = 0, 1, 3, 5, 10$ from below. (b) q dependence of black hole embedding for $m_q = 0.1$ with $q = 0, 1, 3, 5, 10$ from below.

We expect a phase transition between Minkowski and black hole embeddings as we increase temperature. Namely, Minkowski embedding in low temperature will change into black hole embedding in high temperature. In the presence of q , D7 feels repulsive force, therefore we expect that as q increase, phase transition temperature goes up. One may expect that the phase transition might be smoother compared with the case of no instanton charge. One can extract q dependence of phase transition temperature ξ_T^* from the free energy. The case for $m_q = 1$ is drawn in Figure 4.

Now, we will discuss about chiral condensation for this system: it was defined as the slope of D7 brane at asymptotic region. See (3.6). We first fix the temperature and calculate it with different m_q 's. For $q = 0$, D7 brane bends down and its slope at the

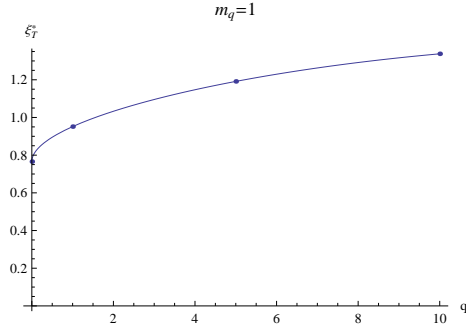


Figure 4: q dependence of phase transition temperature.

asymptotic region is positive and therefore the condensation value is negative. See Figure 5(a). If we turn on q and increase it slowly, the brane bends up relatively very small value of q since the pushing-up effect of q is very effective. Therefore the sign of the condensation flips at small value of q . Also the value of m_q where phase transition occur decreases as q increases.

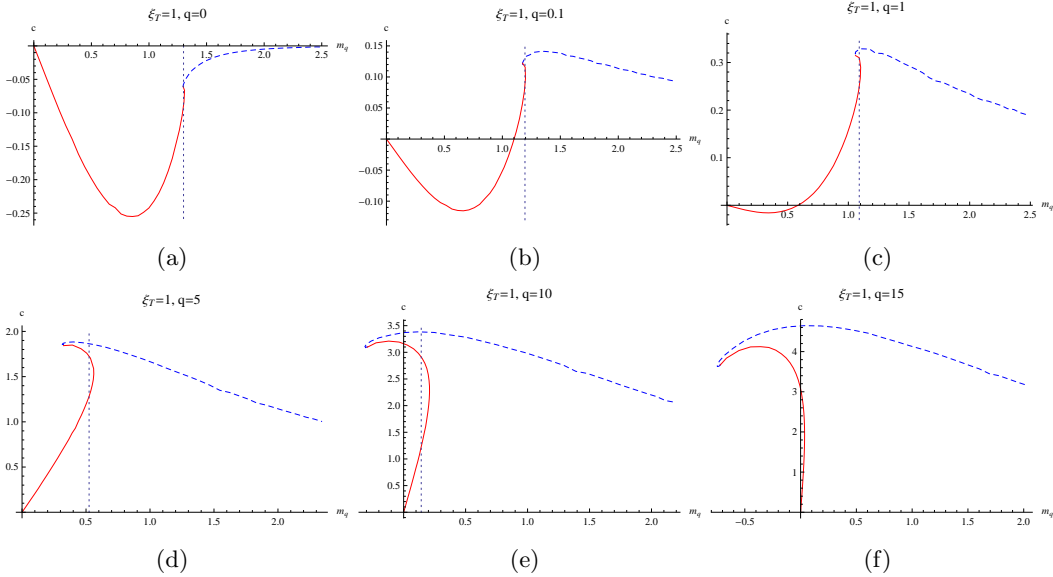


Figure 5: m_q dependence of chiral condensation c for $\xi_T = 1$. Blue dashed line denotes to chiral condensation for Minkowski embedding and red line denotes to black hole embedding. Dotted line indicates phase transition between two embeddings.

As we decrease m_q with fixed q , there is phase transition from Minkowski embedding to black hole embedding at certain value of m_q . See Figure 5. In Figure 5 (e,f) there is range where m_q becomes negative. If we calculate free energy, there is phase transition before m_q becomes negative. Moreover, in Figure 5(f), free energy of Minkowski embedding is always smaller than free energy of black hole embedding. It means that in $m_q \rightarrow 0$ limit, the value of chiral condensation does not vanish, see Figure 6. This is a spontaneous breaking of a

U(1) symmetry which is analogue of the chiral symmetry discussed [20, 21]. Although the relevant symmetry is rotation in x^8, x^9 plane which is not a true chiral symmetry, one can develop the Gellman-Oakes-Renner (GOR) relation [20, 21], which is the purpose of having the chiral symmetry. Therefore from now on we call this as chiral symmetry breaking and we call c as the chiral condensation.

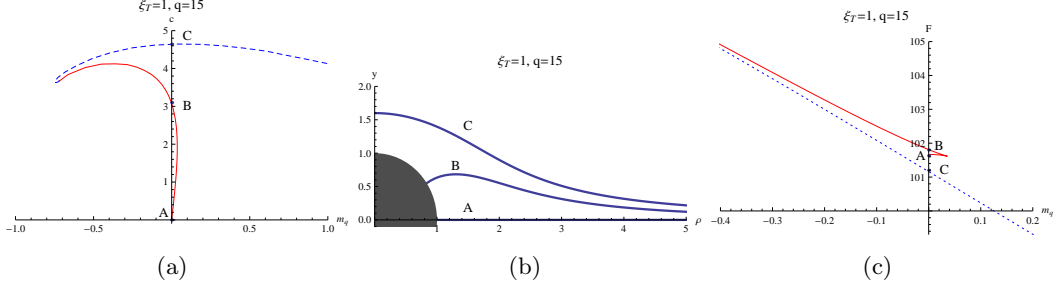


Figure 6: (a) Figure 5(f). A, B and C denote three solution which give zero quark mass. (b) Probe brane embeddings for each case. (c) Free energy as a function of quark mass. C(Minkowski) embedding has minimum energy.

For a given temperature, the chiral symmetry is broken, if q is large enough. The q dependence of chiral symmetry restoring temperature is drawn in Figure 7. When $q \rightarrow 0$, chiral symmetry restoring temperature goes to zero.

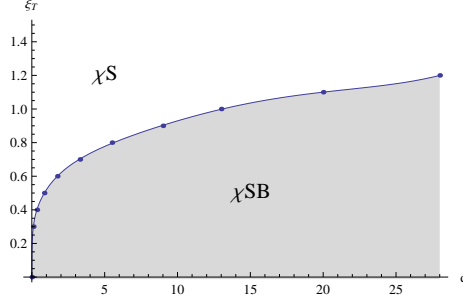


Figure 7: q dependence of chiral symmetry restoring temperature. χSB denotes chiral symmetry breaking phase and χS to chiral symmetry restored phase

4. Chiral symmetry at Finite temperature and finite baryon density

In this section, we discuss D7 brane embedding with finite density using induced metric (2.6). Adding density corresponds to turning on $U(1)$ gauge field $A_t(\rho)$ on D7 brane. The DBI action of D7 brane can be written

$$S_{D7} = -\tau_7 \int dt d\rho \rho^3 e^{\Phi/2} \omega_+^{3/2} \sqrt{e^{\Phi/2} \frac{\omega_-^2}{\omega_+} (1 + \dot{y}^2) - \tilde{F}^2} := \int dt d\rho \mathcal{L}_{D7}, \quad (4.1)$$

where

$$\tau_7 = \mu_7 V_4 \Omega_3, \quad \tilde{F} = 2\pi\alpha' F_{t\rho} \quad (4.2)$$

and dot denotes the derivative with respect to ρ . We used $A_\rho = 0$ gauge. For a fixed charge dynamics, we need Legendre transformation of Lagrangian, which we call ‘Hamiltonian’:

$$\mathcal{H}_{D7} = \tilde{F} \frac{\partial \mathcal{L}_{D7}}{\partial \tilde{F}} - \mathcal{L}_{D7} = \tau_7 \sqrt{e^\Phi \frac{\omega_-^2}{\omega_+} (1 + \dot{y}^2)} \sqrt{\hat{Q}^2 + \rho^6 e^\Phi \omega_+^3}, \quad (4.3)$$

where $\hat{Q} = Q/(2\pi\alpha'\tau_7)$, Q is the number of source charges. Notice that near the horizon, the last factor is dominated by the dilatonic term and the whole action is reduced to the case of $Q = 0$. Therefore the argument for the regularity near the horizon goes exactly the way of the previous section. We can get numerical solution for the equation of motion provided we have proper boundary conditions. The stringy objects corresponding to the sources on D7 brane is the end points of fundamental strings.

Unlike usual black hole background, our background permits the presence of baryon vertex. Therefore there are two way of attaching fundamental strings on D7 brane. One is connecting D7 to the black hole horizon and the other is connecting it to the baryon vertices. Two configurations give different boundary conditions for the D7 brane dynamics. We need to examine which configuration has lower free energy.

4.1 Quark phase

One way to put point electric sources on D7 brane is to add fundamental strings such that one end of strings are on D7 and the other end on black hole horizon. It is equivalent to add freely moving quark in boundary theory because the fundamental strings can move freely on both D7 and horizon. We call it ‘quark’ phase. Since the tension of D7 brane is always smaller than that of fundamental string[15], D7 brane pull down to the horizon.

Regularity at the black hole horizon requests

$$\dot{y}(\rho_{min}) = \tan \theta, \quad (4.4)$$

where θ is polar angle of the position where D7 brane touch the horizon. As discussed in the previous section, the presence of q gives repulsion on probe D7 brane, and it affects its embedding. The q dependence of D7 brane embeddings are drawn in Figure 8 for two different density Q .

From the figure, we can see that as q increases, the repulsion effect on D7 also increases in small density \hat{Q} . However, if \hat{Q} is not small, the brane embedding is less sensitive to q as shown in Figure 8(b). This is because the charge \hat{Q} introduces flux whose electric field energy increases the tension of the D7. That is, the stiffness due to the flux is dominating repulsion due to the q .

In the absence of q , embedding solution which corresponds to $m_q = 0$ is uniquely determined to be the flat embedding, $y(\rho) = 0$ for which value of chiral condensation is automatically zero. However, in the presence of q , there are two different embeddings for the given m_q . For $m_q = 0$, one is trivial with zero chiral condensation c and the other has

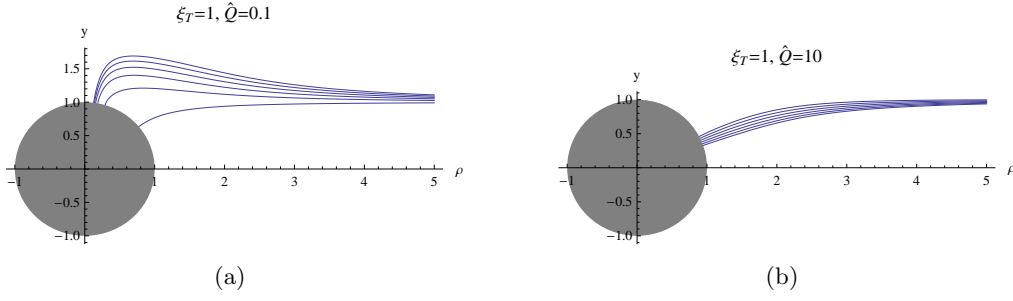


Figure 8: D7 brane embeddings for $m_q = 1$ and $\xi_T = 1$ with $q = 0, 2, 4, 6, 8, 10$ from below for (a) $\hat{Q} = 0.1$, (b) $\hat{Q} = 10$

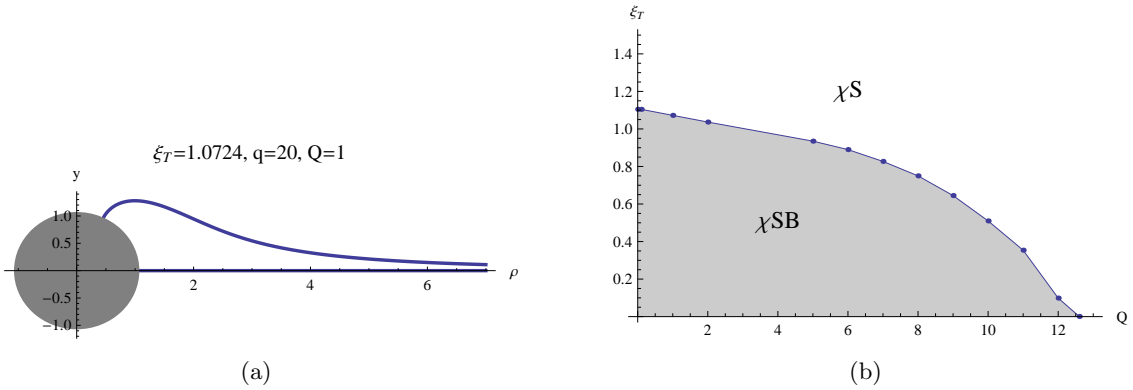


Figure 9: (a) Two embedding solutions with same temperature, density and q . (b) Phase boundary between chiral symmetry breaking and restored phases with $q = 20$.

non-zero chiral condensation as we can see in Figure 9(a). The solution with non-zero c exists in low temperature and small density region. In large density region, only $y = 0$ is the solution. Actually we found that there is a phase transition between the two embeddings in certain temperature and density. The phase diagram is presented in Figure 9(b). As q increase the phase boundary expands toward larger temperature and density region. See Figure 10. This is natural since the chiral symmetry breaking is caused by the effect of gluon condensation q , as we have seen in Figure 2¹.

In Figure 8, D7 embedding for non-zero m_q is drawn. In this case, behavior of D7 brane embedding is similar to black hole embedding with $q = 0$. Due to the non-zero value of $y(\infty) \sim m_q$, chiral symmetry is explicitly broken. However, it is known that there is first order phase transition in black hole background between two quark phases in small density region[14, 15]. This phase transition line finishes at certain density and temperature. At this point, the order of phase transition is second. As q increase, the phase phase boundary line moves upward in (T, Q) plane. See Figure 11.

¹This phenomenon is very similar when we turn on the magnetic field on probe brane [25] in black D3 brane background. But in that case, the magnetic field cannot affect the background geometry and the interpretation of magnetic field also different.

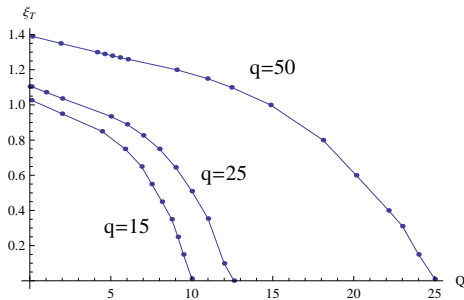


Figure 10: phase diagram of chiral symmetry restoration within quark phase for $q=15, 25$ and 50 .

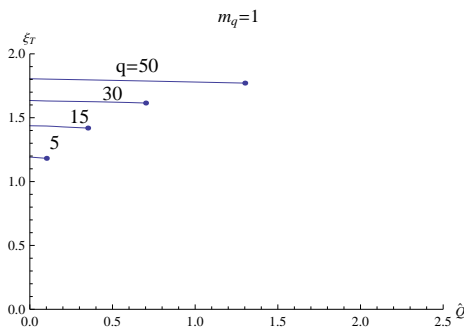


Figure 11: q dependence of phase transition between two quark phase for fixed $m_q = 1$. These phase transition lines end with second order phase transition point.

There is an issue about thermodynamical instability around first order phase transition point in black hole background [14, 15]: chemical potential decreases as density increases, that is, $\partial\mu/\partial Q < 0$. But in the presence of q , this instability can be cured as we will discuss later.

4.2 Baryon phase

In this section, we study a baryon vertex in the D3/D-instanton background. Baryon vertex is originally proposed in [2]. Near horizon geometry of black D3 brane is $AdS_5 \times S^5$. If we wrap spherical D5 brane on S^5 , due to the Chern-Simons interaction between R-R five form field strength and D5 brane world volume, $U(1)$ gauge field is induced on D5 brane world volume and to cancel these fluxes we need to put N_c fundamental strings on D5 brane. In asymptotic region, this object looks like bound state of N_c fundamental string or quark. We call this object to ‘baryon vertex’.

As discussed in [4], however, in Schwartzschild type black hole background does not allow compact D5 brane as a solution of equation of motion of DBI action. Therefore, the quark phase is only physical in finite temperature system. But, in the D3/D-instanton background, compact D5-brane with N_c fundamental strings can be formed even in the black hole background.[10]. By connecting baryon vertex and probe D7 brane [4], we can discuss thermodynamics of finite density and temperature system.

To study properties of baryon vertex, we rewrite the 10 dimensional metric (2.3);

$$ds^2 = e^{\Phi/2} \left[\frac{r^2}{R^2} (f(r)^2 dt^2 + d\vec{x}^2) + R^2 \left(\frac{d\xi^2}{\xi^2} + d\theta^2 + \sin^2 \theta d\Omega_4^2 \right) \right], \quad (4.5)$$

We take (t, θ_α) as world volume coordinates of a compact D5 brane, and turn on the $U(1)$ gauge field on it to have $F_{t\theta} \neq 0$. As the ansatz for the embedding of compact D5, we assume the $SO(5)$ symmetry so that position of D5 brane and gauge field depend only on θ i.e. $\xi = \xi(\theta)$, $A_t = A_t(\theta)$, where θ measure the polar angle of S^5 from the north pole. The induced metric on D5 brane is

$$ds_{D5}^2 = e^{\Phi/2} \left[\frac{r^2}{R^2} f^2 dt^2 + R^2 \left(\frac{\xi'^2}{\xi^2} + 1 \right) d\theta^2 + R^2 \sin^2 \theta d\Omega_4^2 \right], \quad (4.6)$$

where $\xi' = d\xi/d\theta$. The DBI action for single D5 brane with N_c fundamental string can be written as

$$\begin{aligned} S_{D5} &= -\mu_5 \int e^{-\Phi} \sqrt{-\det(g + 2\pi\alpha' F)} + \mu_5 \int A_{(1)} \wedge G_{(5)} \\ &= \tau_5 \int dt d\theta \sin^4 \theta e^\Phi \left[-\sqrt{e^\Phi \frac{\omega_-^2}{\omega_+} (\xi^2 + \xi'^2) - \tilde{F}^2 + 4\tilde{A}_t} \right] \\ &= \int dt d\theta \mathcal{L}_{D5}, \end{aligned} \quad (4.7)$$

where

$$\tau_5 = \mu_5 \Omega_4 R^4 r_T, \quad \tilde{F} = 2\pi\alpha' F_{t\theta}, \quad \tilde{A}_t = 2\pi\alpha' A_t. \quad (4.8)$$

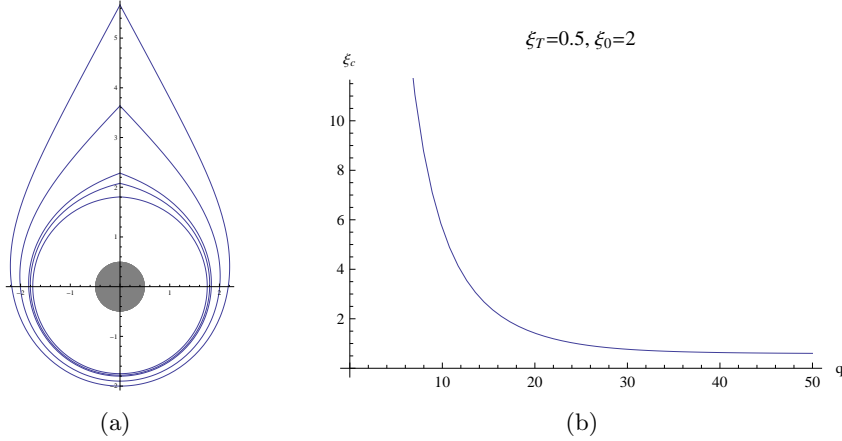


Figure 12: (a) ξ_0 dependence of D5 brane embeddings with $q = 10$, $\xi_T = 0.5$. Gray disk denotes to black hole. (b) q dependence of tip of D5 brane(ξ_c).

After solving the equation of motion for gauge field and substituting it to the Lagrangian density, we can get ‘Hamiltonian’ density of D5 brane,

$$\mathcal{H}_{D5} = \tau_5 \sqrt{\frac{e^\Phi \omega_-^2}{2 \omega_+} (\xi'^2 + \xi^2)} \sqrt{\hat{D}(\theta)^2 + \sin^8 \theta}, \quad (4.9)$$

where

$$\hat{D}(\theta) = -\frac{3}{2}\theta + \frac{3}{2}\sin\theta\cos\theta + \sin^3\theta\cos\theta. \quad (4.10)$$

Here, we consider all fundamental strings are attached at north pole. For more detail, see Appendix B.

The equation of motion for (4.9) depends on two parameters q , ξ_T and two initial condition $\xi(\theta = 0) = \xi_0$, $\xi'(\theta = 0) = 0$. Here we set $\theta = 0$ is south pole of D5 brane. For a given value of expectation value of gluon condensation(q) and temperature(ξ_t), we can get numerical solution in terms of ξ_0 . The set of numerical solutions in ξ plane is drawn in Figure 12(a). In this figure, a cusp appears at $\theta = \pi$ on where N_c fundamental strings are attached. But these closed D5 brane does not exist in whole value of q and ξ_t . When the value of q decrease, the position of tip (we denote it to ξ_c) increase and $q \rightarrow 0$ limit, the tip of D5 brane goes to infinity, 12(b). It is consistent with the fact that the usual Schwartzschild black hole background does not allow baryon vertex. We also check that the baryon vertex solution does not exist at high temperature.

As we discussed in [4], we can add D7 brane at the tip of D5 brane with force balance condition[26],

$$y'(\rho = 0) = \frac{\xi'_c}{\xi_c}, \quad (4.11)$$

where ξ_c and ξ'_c denote to the position and slop of D5 brane at $\theta = \pi$. For details, see Appendix C. The full configurations of D7/D5 brane embeddings with certain value of q and density are drawn in Figure 13. We call this phase as 'baryon phase' because in this phase the physical object is baryon vertex. From this figure, we can see that in the presence of baryon vertex, the slope of probe brane in asymptotic region is always non-zero. It means that in baryon phase, chiral symmetry is always broken. We found that the embedding corresponding to the baryon phase does not exist at high temperature.

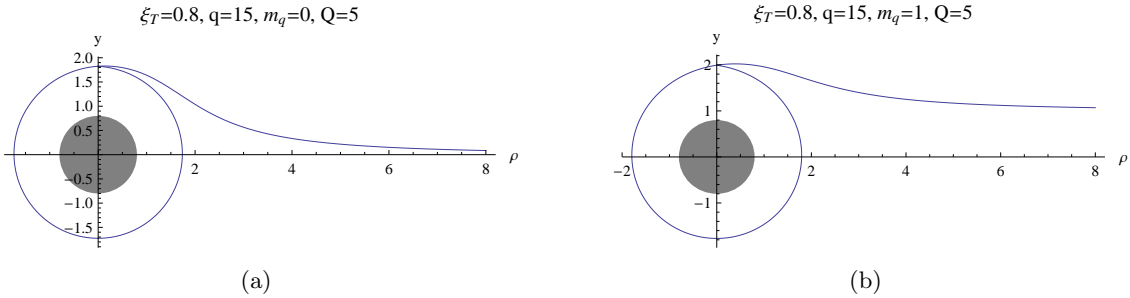


Figure 13: D7 brane embeddings for $\xi_T = 0.8$, $\tilde{Q} = 5$ with (1) $m_q = 0$ (b) $m_q = 1$

5. Phase Transition

As we discussed in previous section, two kinds of embeddings can exist in finite temperature. They correspond to two phases: black hole embedding corresponds to the quark phase and Minkowski embedding corresponds to the baryon phase. Quark phase can exist whole

temperature region while baryon phase can exist only at low temperature region. In our model, the baryon phase exists if temperature is low enough regardless of how high is the density. However, in low temperature, quark phase is also possible. To determine which is the physical phase, we need to compare the free energies of two systems. There are two ensembles we can choose, one is canonical ensemble where density is control parameter. In canonical ensemble we can determine physical phase by comparing free energy. Since we need to determine the configuration in a fixed value of the charge we need Legendre transformed action which we call ‘Hamiltonian’, although it is not the time translation generator. The other one is grand canonical ensemble where chemical potential is control parameter. In this case we have to calculate grand potential which is value of DBI action.

5.1 Canonical ensemble

To determine physical solution in canonical ensemble, we have to compare free energies of two phases. Free energy of quark phase is given by integrating Hamiltonian (4.3) density for the embeddings,

$$\mathcal{F}_{\text{quark}}(\hat{Q}) = \tau_7 \int_{\rho_{\min}}^{\infty} d\rho \hat{\mathcal{H}}_{D7}(\hat{Q}) \Big|_{\text{quark phase}}, \quad (5.1)$$

where $\hat{\mathcal{H}}_{D7} = \mathcal{H}_{D7}/\tau_7$ (we introduce it for convenience). Here, we regularized free energy by subtracting energy of flat D7 brane.

On the other hand, baryon phase needs compact D5 brane, called baryon vertex operator. Since each D5 should have N_c quarks, their number is related to the quark number by $N_B = Q/N_c$. The total free energy in baryon phase can be obtained by adding energy of D5 brane to that of D7 brane:

$$\begin{aligned} \mathcal{F}_{\text{baryon}}(\hat{Q}) &= \tau_7 \int d\rho \hat{\mathcal{H}}_{D7}(Q) \Big|_{\text{baryon phase}} + \frac{Q}{N_c} \tau_5 \int d\theta \hat{\mathcal{H}}_{D5} \\ &= \tau_7 \left[\int d\rho \hat{\mathcal{H}}_{D7}(\hat{Q}) \Big|_{\text{baryon phase}} + \frac{2}{3\pi} \hat{Q} \int d\theta \hat{\mathcal{H}}_{D5} \right]. \end{aligned} \quad (5.2)$$

By comparing the value of (5.1) and (5.2), we can determine which phase is physically favored. As we discussed in previous section, there are two phases in quark phase, which is true also in massless quark case. One is quark phase with broken chiral symmetry and the other one is phase with chiral symmetry restored. The density dependences of free energy in massless quark case are drawn in Figure 14. In the figure, we plotted \tilde{F} which is defined as $\tilde{F} = F - \alpha(T)Q$ to visualize the difference of the free energies of different phases. One should notice that all the free energies monotonically increase as function of density, although the figure does not show that due to the subtraction of $\alpha(T)Q$.

At low temperature, the free energy of baryon phase is always lower than that of quark phase for all density region, see Figure 14(a). It means that the baryon phase is physical at low temperature. As temperature increase, the free energy lines change drastically, see Figure 14(b). At temperature $\xi_t = 0.16$, the free energy of baryon phase is lowest in low density region. As density increase, there is phase transition between baryon phase and quark phase with broken chiral symmetry (first vertical line in 14(b)). After the baryon

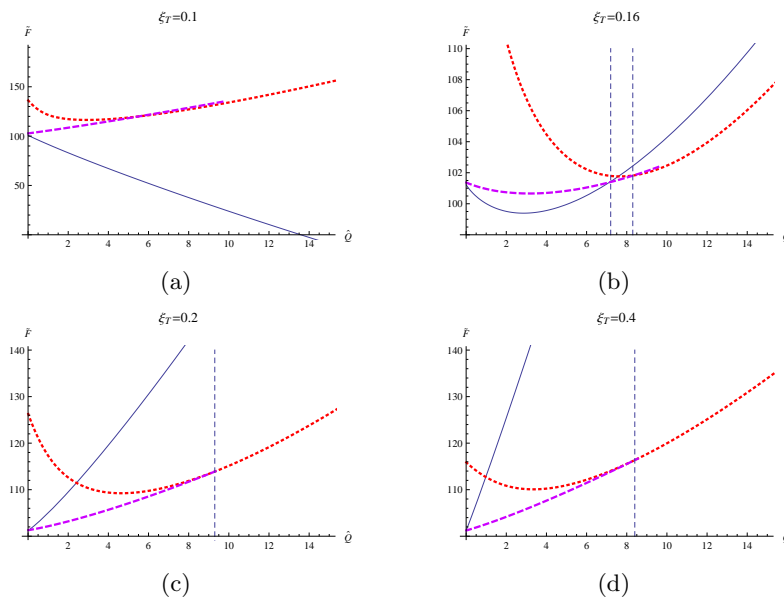


Figure 14: Density dependence of free energy for massless quark case with $q = 15$. To visualize the difference of free energy, we plotted \tilde{F} which is defined as $\tilde{F} = F - \alpha(T)Q$ for some $\alpha(T)$. Solid line is for baryon phase, red dotted line is for chiral symmetry restored quark phase and dashed purple line is for quark phase with chiral symmetry broken. Vertical dotted line denotes phase transition point.

to quark phase transition, there is another phase transition between quark phases: from broken to restored chiral symmetry quark phase. At higher temperature, the free energy of quark phase is always smaller than that of baryon phase. But there is a phase transition from chiral symmetry broken phase to chiral symmetry restored phase at certain density. See Figure 14(c), (d). The chiral phase transition between two quark phases coincide with the result of previous section, Figure 10. Of course, at high enough temperature, the chiral symmetry restored quark phase is the only physical phase. These are summarized in the phase diagram drawn in Figure 15.

This phase diagram has rich structure. At low temperature, baryon phase is always physical one in all density region. And chiral symmetry is always broken in this phase. However, as we increase temperature, phase transition appears differently depends on density. At low density, as temperature increase, baryon phase changes into quark phase but chiral symmetry is still broken. If we increase temperature more, then there is chiral symmetry restoration transition in quark phase. On the other hand, at high density, as we increase temperature, baryon/quark phase transition and chiral phase transition appears at the same time.

We find that the baryon/quark phase transition temperature decreases as density increase. However, the decreasing rate is too slow so that phase transition temperature looks like constant in the figure. The value of q also affect phase transition. As q increase, both phase boundaries move up to larger temperature and larger density region maintaining the overall shape. See Figure 15(b). Notice that our phase diagram is very similar to the ones

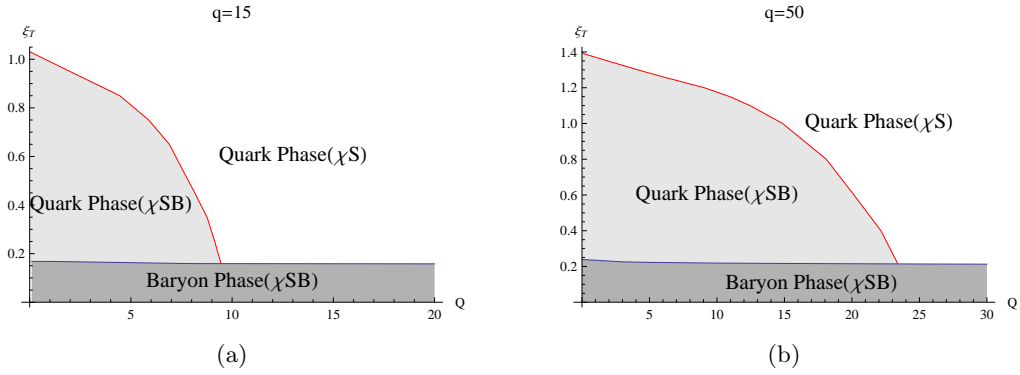


Figure 15: Density dependence of phase transition temperature between quark phase and baryon phase (a) with $q = 15$, (b) with $q = 50$.

for Sakai-Sugimoto model studied in [27], where the baryon phase should be replaced by the soliton geometry. Notice that in our model, there is no Hawking Page transition since there is no scale other than the temperature and the dilaton contribution is precisely canceled by that of the axion. Our baryon phase is still in the black hole geometry therefore the dynamic origin is very different.

In the case of $m_q \neq 0$, chiral symmetry is explicitly broken so that we might expect that there is only baryon/quark phase transition. However, as we discussed in previous section, there is another phase transition in quark phase. Look at the short line at the up-left region of the phase diagram in Figure 16. It is for $m_q = 1$.

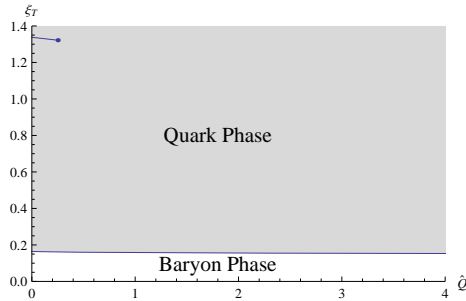


Figure 16: Density dependence of phase transition temperature between quark phase and baryon phase for $m_q = 1$ and $q = 20$.

As we decreases the quark mass, the end point of the phase boundary extends to higher density and lower temperature region so that when $m_q \rightarrow 0$, we recover the phase diagram drawn in Figure 15. Actually the line becomes long very fast when m_q gets to the near zero value. Contrarily for $q = 0$, the line for the transition from black hole embedding (BHE) to another BHE exist only in very small density region and it disappear when m_q goes to zero. Therefore this is very characteristic feature caused by the gluon condensation q .

5.2 Relation between chemical potential and density

Equations of states which are the relations between thermodynamically conjugate variables like chemical potential/density, quark mass/chiral condensation e.t.c. play important role to understand phase structure. In this section, we will discuss the equation of state describing the relation between chemical potential and density. Thermodynamically chemical potential is defined as derivative of free energy with respect to density,

$$\mu = \frac{\partial \mathcal{F}}{\partial Q}. \quad (5.3)$$

In quark phase, we can get

$$\begin{aligned} \mu_{quark} &= \frac{\partial \mathcal{F}_{quark}}{\partial Q} \\ &= \frac{1}{2\pi\alpha'} \int_{\rho_{min}}^{\infty} \frac{\partial \hat{\mathcal{H}}_{D7}}{\partial \hat{Q}} \\ &= \int_{\rho_{min}}^{\infty} d\rho \partial_{\rho} A_t = A_t(\infty) - A_t(\rho_{min}). \end{aligned} \quad (5.4)$$

In this case, $A_t(\rho_{min}) = 0$ because ρ_{min} is black hole horizon. It is consistent with usual definition of chemical potential (value of A_t field) from AdS/CFT correspondence. On the other hand, the free energy of baryon phase contains mass of baryon vertex, chemical potential should have mass of source.

$$\begin{aligned} \mu_{baryon} &= \frac{\partial \mathcal{F}_{baryon}}{\partial Q} \\ &= \frac{1}{2\pi\alpha'} \int_{\rho_{min}}^{\infty} \frac{\partial \hat{\mathcal{H}}_{D7}}{\partial \hat{Q}} + \frac{1}{2\pi\alpha'} \frac{2}{3\pi} \int d\theta \hat{\mathcal{H}}_{D5} \\ &= A_t(\infty) - A_t(\rho_{min}) + \frac{1}{N_c} \int d\theta \mathcal{H}_{D5}. \end{aligned} \quad (5.5)$$

The last term in (5.5) the baryon mass divided by N_c , which is the constituent quark mass. Therefore, the chemical potential contains mass of the source. In quark phase, the source is the fundamental strings. For the blackhole embedding, D7 brane touches the black hole (BH) horizon and the fundamental strings are replaced by deformation of D7 brane. Therefore the energy of fundamental strings is contained in that of D7 brane. That's why there is no source term, the analogue of the last term in the eq.(5.5), in the chemical potential of the quark phase. The density dependences of chemical potential for $m_q = 0$ embedding are drawn in Figure 17. We can see that chemical potentials monotonically increase as density increases for any phases. Therefore, there is no thermodynamical instability in $m_q = 0$ case.

The free energy and chemical potential with finite quark mass as functions of density are drawn in Figure 18. Figure 18(a) shows density dependence of free energy at finite temperature with $q = 50$ and $m_q = 1$. At certain density there is phase transition in quark phase. In usual AdS Schwarzschild background without q , there is a thermodynamical instability associated with the negative slope branch of the μ - Q diagram. But in Figure

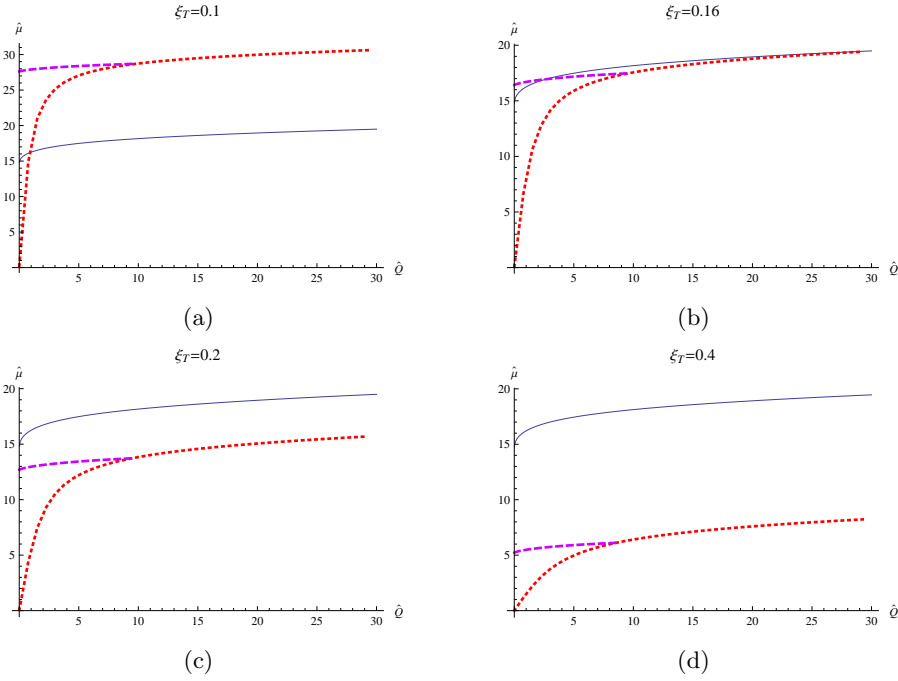


Figure 17: Density dependence of chemical potential for $m_q = 0$. Red dotted line denotes chemical potential for quark phase with chiral symmetry and purple dashed line is for quark phase with broken chiral symmetry. The solid line denotes baryon phase.

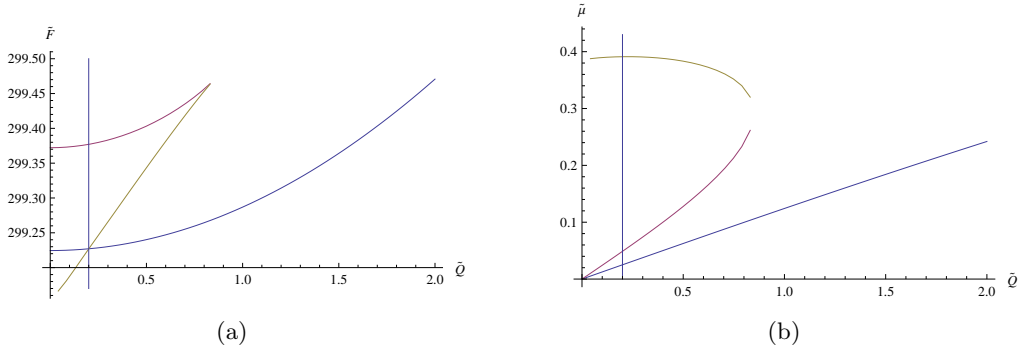


Figure 18: (a) Free energy as a function of density in certain temperature for $m_q = 1$. (b) Density dependence of chemical potential, $\tilde{\mu} = 2\pi\alpha'\mu$. In both figure $\xi_T = 1.3$, $q = 50$.

18(b), we can see that chemical potential increases at low density and phase transition happens before chemical potential begin to decrease. Therefore, chemical potential for physical state always increase monotonically as density increase ($\partial\mu/\partial Q > 0$), hence there is no thermodynamical instability.

As temperature decreases, both quark phase and baryon phase exist and the shape of chemical potential is monotonic as function of the density in both phases which is similar to Figure 17.

5.3 Grand canonical ensemble

In this section, we will discuss the system with grand canonical ensemble. Grand potential is thermodynamically defined as

$$\Omega = \mathcal{F} - \mu Q. \quad (5.6)$$

From definition of ‘Hamiltonian density and number density, grand potential for quark phase can be written as

$$\begin{aligned} \Omega_{quark} &= \mathcal{F}_{quark} - \mu_{quark} Q \\ &= \int \tilde{F} \frac{\partial \mathcal{L}_{D7}}{\partial \tilde{F}} \Big|_{quark \ phase} - \int \mathcal{L}_{D7} \Big|_{quark \ phase} - \int \tilde{F} \tilde{Q} \\ &= - \int \mathcal{L}_{D7} \Big|_{quark \ phase}. \end{aligned} \quad (5.7)$$

The last term in (5.7) is nothing but value of on-shell DBI action for black hole phase. It is obvious because ‘Hamiltonian density’ is defined by Legendre transformation of DBI action. Grand potential for baryon phase becomes

$$\begin{aligned} \Omega_{baryon} &= \mathcal{F}_{baryon} - \mu_{baryon} Q \\ &= \int \mathcal{H}_{D7} \Big|_{baryon \ phase} + \frac{Q}{N_c} \int \mathcal{H}_{D5} - \left(\int \tilde{F} \tilde{Q} + \frac{Q}{N_c} \int \mathcal{H}_{D5} \right) \\ &= - \int \mathcal{L}_{D7} \Big|_{baryon \ phase}. \end{aligned} \quad (5.8)$$

We can see that energy of source in free energy canceled by one in chemical potential, final form of grand potential is value of DBI action of D7 brane for baryon phase. D5 part does not contribute to grand potential.

In the massless quark case ($m_q = 0$), the grand potentials of quark and baryon phase are drawn in Figure 19. In each case of the that figure, chemical potential start from non-zero value as one can see in Figure 17. It implies that if the chemical potential is not large enough to the energy of particle, no particle can be created. Therefore, the system remains as vacuum until chemical potential reach to the energy of particle in the system. Therefore the value of the chemical potential should be identified as the constituent quark mass. Naturally the difference in the chemical potential in baryon phase and that in the realized quark phase (between the two quark phases) can be identified as the binding energy. The density dependence of the quark mass is plot in figure 19. The phase transition point can be identified precisely as the point the binding energy is 0. This point is of course the point where baryons melt. The melting point in temperature-density plane is nothing but our phase diagram.

From the figure Figure 19, one can easily read off the critical chemical potential value points as one increases the temperature.

In the case of finite quark mass, chiral symmetry is always broken similar to the canonical ensemble. We have only two phases, the baryon phase and quark phase. However, we find that the density dependence of chemical potential and the chemical potential dependence of grand potential behave similarly to the massless case except the absence of chiral

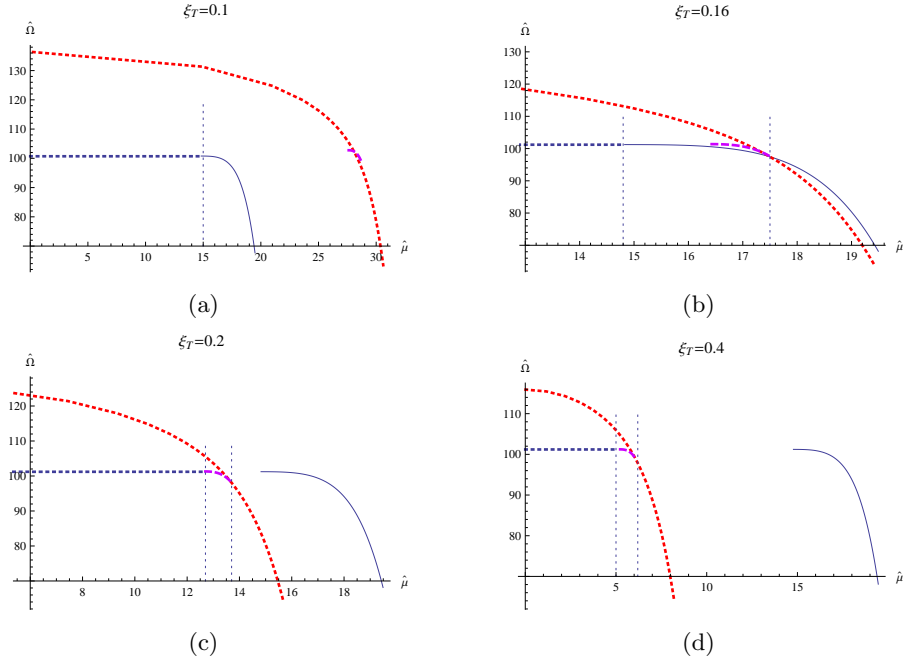


Figure 19: Chemical potential dependence of grand potential ($m_q = 0$ and $q = 15$). Red dotted line denotes to grand potential for chiral symmetry restored quark phase purple dashed line to grand potential for quark phase without chiral symmetry and solid line to baryon phase

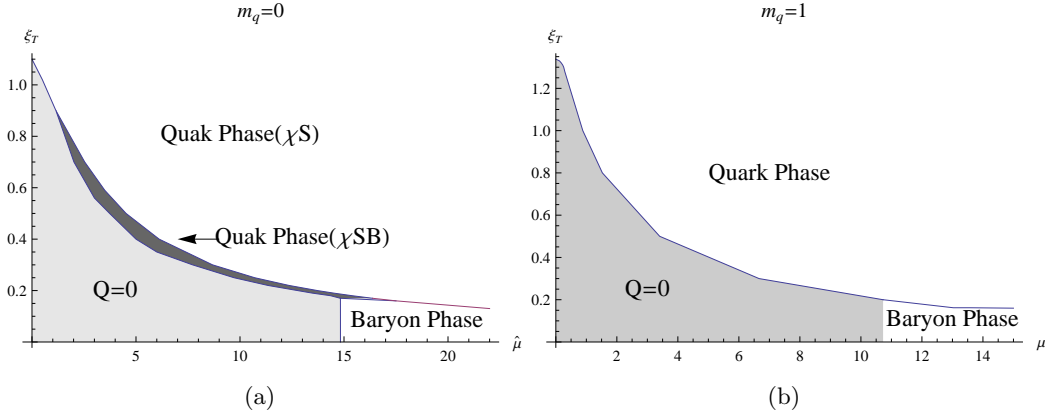


Figure 20: Phase boundary in grand canonical ensemble in the case of (a) $m_q = 0$, (b) $m_q = 1$.

phase transition. The phase structure based on above discussion is drawn in Figure 20. Similar to phase diagram in canonical ensemble, the temperature of phase transition between quark and baryon phase is almost constant. We also find the transition in quark phase in small density region, but this line is not shown in this diagram.

5.4 Chiral condensation

One of the most important observable in QCD is the chiral condensation (CC) and its

density dependence. It measures the dynamical mechanism for creating the mass of the hadrons. Figure 21 shows the density dependence of the chiral condensation. In the baryon phase, chiral symmetry is always broken and there is a quark phase where chiral symmetry is broken. Our result shows that CC is increasing in baryon phase and decreasing in the relevant quark phase.

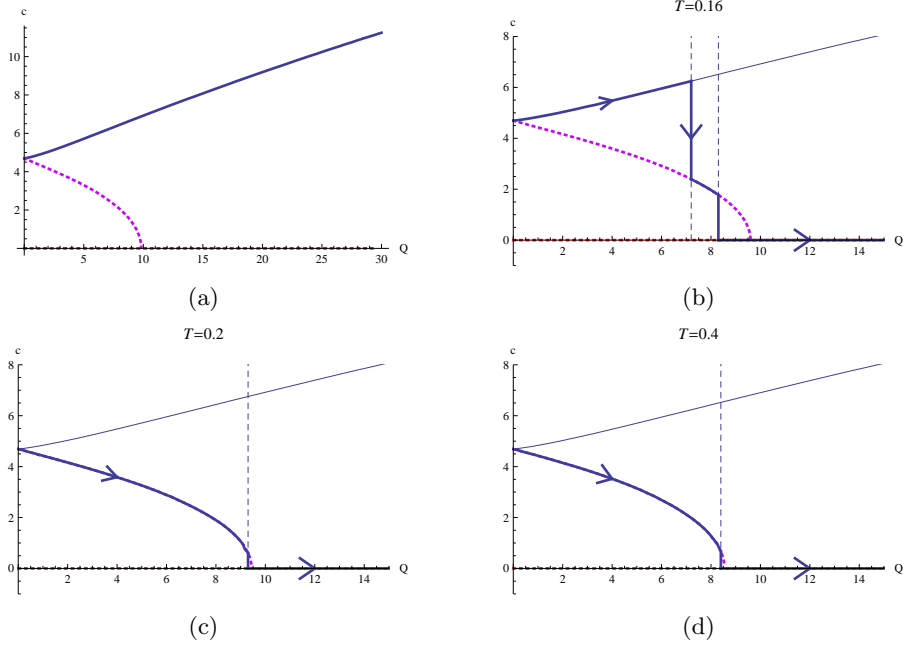


Figure 21: Density dependence of the value of chiral condensation $\langle \bar{q}q \rangle$ for massless quark case with $q = 15$. Thick line indicates physical phase from free energy and there is phase transition along vertical dashed line.

6. Summary and Discussion

In this paper, we study phase structure of a holographic QCD based on D3/D-instanton background. The phase transition here is for confinement/deconfinement of quark not the gluons. While the Hawking Page transition in usual AdS/CFT correspondence describes the dynamics of the gluon, confinement/deconfinement phase transition of quarks are determined from the interaction between the geometry and the compact brane dynamics. Namely it is question of existence of the baryon vertex. The D3/D-instanton background have quasi-confining nature as defined in the introduction. In zero quark mass case, there is a chiral transition in quark phase. The number of D-instanton, identified as the expectation value of gluon condensation played, essential role in breaking the chiral symmetry. The phase boundary is depends on value of q .

A few remarks are in order:

The first one is on the assumption that there is no Hawking-Page transition. Main reason is that the geometric transition should be discussed in the Einstein frame, where

dilaton action is cancelled by that of axion therefore we can not find any effect of the dilaton condensation scale in bulk free energy level. Therefore it is completely the same as the D3 brane without D-instanton. However all the probe D-brane dynamics is affected by the presence of the dilaton factor. That is why we get non-trivial result. This is interesting and subtle point and in the main sections we just assumed that there is no Hawking-Page transition.

Second one is about the role of the Chern-Simons term. In ref. [9], the authors introduced Chern-Simons term such that it cancel out the dilaton effect of the brane embedding dynamics. However, we could not find solution with such behavior. We found that the Chern-Simons term is a total derivative so that it can contribute to the charge but not to the equation of motion. This allows us the non-trivial effect of the gluon condensation on the embedding of D7 brane as well as on that of D5.

The third one is that due to the probe nature of the embedding dynamics, our calculation is not trusted in extreme high density regime. One need to take care of the backreaction of the geometry.

The 4th is the Euclidean nature and duality in such background. For the Euclidean configuration, there is no state/geometry correspondence. However, gauge gravity duality is still there. The correspondence of D-instanton in type IIB and Yang-Mill theory instanton was discussed in [28] as well as many other papers. The relation of AdS/CFT and multi-instanton gauge theory is considered in well known works of Dorey et.al. [29]. So the gauge theory dual of the uniform distribution of such D-instanton is not hard to imagine and it should be the Yang-Mill theory with uniform distribution of instanton charge.

The 5th is the Infra-red singularity. The background has the IR singularity since the dilaton factor has log singularity at the horizon. Usually one need to prevent any D-brane probe to approach such singular region. Also this makes the bulk action divergent and we would need IR cut off. However, in our background, both the bulk gravity action as well as the DBI action are regular at the horizon. There is no divergence. There are reasons for this. i) The finite temperature version has a regular horizon and the essential singularity is hidden in the horizon. ii) The finiteness of the bulk action is partly due to the supersymmetric construction of the action and the ansatz eq.(3.1) by which the action of dilaton is cancelled precisely by that of axion. iii)The finiteness of the probe brane action is due to detailed structure of DBI action. Looking at eq. (4.7), the log divergence of dilaton factor e^{Φ} is cancelled by the presence of the ω_- factor, which has a zero. The thermodynamics is based on the calculation of the DBI action for the actual configuration of the brane. Speaking more physically, the background act net repulsive force to the D-brane which perform the dynamic censorship and gives finite values of DBI action.

In the background with $q = 0$, the meson spectral function does not have interesting feature. But due to the repulsive nature of the force acting on the probe brane, there is some reason to expect non-trivial spectral behavior in this case. It would be very interesting to calculate the meson spectrum in the chiral symmetry broken quark phase.

Acknowledgments

This work was supported by the National Research Foundation of Korea(NRF) grant funded by the Korea government(MEST) through the Center for Quantum Spacetime(CQUeST) of Sogang University with grant number 2005-0049409. The work of YS and SJS was supported by Mid-career Researcher Program through NRF grant(No. 2010-0008456). The work of MK was supported in part by KRF-2007-313- C00150, WCU Grant No. R32-2008-000-101300.

A. Chern-Simons term

We will put probe D7 brane, then 8-form field from hodge dual of axion can interact with D7 brane world volume. We check it in zero temperature limit and extend to finite temperature case.

In the limit $T \rightarrow 0$, (2.2) becomes

$$\begin{aligned} ds &= e^{\Phi/2} \left\{ \frac{r^2}{R^2} (-dt^2 + d\vec{x}^2) + \frac{R^2}{r^2} (dr^2 + r^2 d\Omega_5^2) \right\} \\ e^\Phi &= 1 + \frac{q}{r^4}, \quad \chi = -e^{-\Phi} + \chi_\infty. \end{aligned} \quad (\text{A.1})$$

We are interested in interaction between dual field of axion and probe D7 brane, we change the metric into the direction along and perpendicular to D7 brane,

$$ds = e^{\Phi/2} \left\{ \frac{r^2}{R^2} (-dt^2 + d\vec{x}^2) + \frac{R^2}{r^2} (d\rho^2 + \rho^2 d\Omega_3^2 + dy^2 + y^2 d\phi^2) \right\}, \quad (\text{A.2})$$

where $r^2 = \rho^2 + y^2$. To get dual field, we introduce vielbein

$$\begin{aligned} e^{\tilde{t}} &= e^{\Phi/4} \frac{r}{R} dt, \quad e^{\tilde{x}_i} = e^{\Phi/4} \frac{r}{R} dx_i, \quad e^{\tilde{\rho}} = e^{\Phi/4} \frac{R}{r} d\rho, \\ e^{\tilde{\Omega}_3} &= e^{\Phi/4} \frac{R}{r} \rho d\Omega_3, \quad e^{\tilde{y}} = e^{\Phi/4} \frac{R}{r} dy, \quad e^{\tilde{\phi}} = e^{\Phi/4} \frac{R}{r} y d\phi, \end{aligned} \quad (\text{A.3})$$

where tilde denotes to flat index. The field strength for axion field is

$$\begin{aligned} F_{(1)} &= d\chi = \frac{\partial\chi}{\partial r} dr \\ &= e^{-\Phi} \frac{\partial\Phi}{\partial\rho} d\rho + e^{-\Phi} \frac{\partial\Phi}{\partial y} dy \\ &= e^{-5\Phi/4} \frac{\partial\Phi}{\partial\rho} \frac{r}{R} e^{\tilde{\rho}} + e^{-5\Phi/4} \frac{\partial\Phi}{\partial y} \frac{r}{R} e^{\tilde{y}}. \end{aligned} \quad (\text{A.4})$$

Hodge dual of this field strength is

$$\begin{aligned} F_{(9)} &= \frac{1}{9!} e^{-5\Phi/4} \frac{\partial\Phi}{\partial\rho} \frac{r}{R} \epsilon_{\tilde{t}\tilde{x}_i\tilde{\Omega}_3\tilde{y}\tilde{\phi}}^{\tilde{\rho}} e^{\tilde{t}} \wedge e^{\tilde{x}_i} \wedge e^{\tilde{\Omega}_3} \wedge e^{\tilde{y}} \wedge e^{\tilde{\phi}} \\ &\quad + \frac{1}{9!} e^{-5\Phi/4} \frac{\partial\Phi}{\partial y} \frac{r}{R} \epsilon_{\tilde{t}\tilde{x}_i\tilde{\Omega}_3\tilde{\rho}\tilde{\phi}}^{\tilde{y}} e^{\tilde{t}} \wedge e^{\tilde{x}_i} \wedge e^{\tilde{\rho}} \wedge e^{\tilde{\Omega}_3} \wedge e^{\tilde{\phi}} \end{aligned}$$

$$\begin{aligned}
&= e^\Phi \frac{\partial \Phi}{\partial \rho} \rho^3 y dt \wedge d\vec{x} \wedge d\Omega_3 \wedge dy \wedge d\phi \\
&\quad - e^\Phi \frac{\partial \Phi}{\partial y} \rho^3 y dt \wedge d\vec{x} \wedge d\Omega_3 \wedge d\rho \wedge d\phi \\
&= \frac{\partial e^\Phi}{\partial \rho} \rho^3 y dt \wedge d\vec{x} \wedge d\Omega_3 \wedge dy \wedge d\phi \\
&\quad - \frac{\partial e^\Phi}{\partial y} \rho^3 y dt \wedge d\vec{x} \wedge d\Omega_3 \wedge d\rho \wedge d\phi,
\end{aligned} \tag{A.5}$$

where we are using the convention

$$\epsilon_{\tilde{t}\tilde{x}_i\tilde{\rho}\tilde{\Omega}_3\tilde{y}\tilde{\phi}} = +1. \tag{A.6}$$

By substituting e^Φ , we get

$$\begin{aligned}
F_{(9)} &= -\frac{4q\rho^4 y}{(\rho^2 + y^2)^3} dt \wedge d\vec{x} \wedge d\Omega_3 \wedge dy \wedge d\phi \\
&\quad + \frac{4q\rho^3 y^2}{(\rho^2 + y^2)^3} dt \wedge d\vec{x} \wedge d\Omega_3 \wedge d\rho \wedge d\phi.
\end{aligned} \tag{A.7}$$

Now, we want to get 8-form potential such that

$$F_{(9)} = dC_{(8)}. \tag{A.8}$$

Assuming

$$\begin{aligned}
C_{(8)} &= f(\rho, y, \phi) dt \wedge d\vec{x} \wedge d\Omega_3 \wedge dy \\
&\quad + g(\rho, y, \phi) dt \wedge d\vec{x} \wedge d\Omega_3 \wedge d\rho,
\end{aligned} \tag{A.9}$$

we get

$$\begin{aligned}
dC_{(8)} &= \frac{\partial f}{\partial \phi} dt \wedge d\vec{x} \wedge d\Omega_3 \wedge dy \wedge d\phi \\
&\quad - \frac{\partial f}{\partial \rho} dt \wedge d\vec{x} \wedge d\Omega_3 \wedge d\rho \wedge dy \\
&\quad + \frac{\partial g}{\partial \phi} dt \wedge d\vec{x} \wedge d\Omega_3 \wedge d\rho \wedge d\phi \\
&\quad + \frac{\partial g}{\partial y} dt \wedge d\vec{x} \wedge d\Omega_3 \wedge d\rho \wedge dy.
\end{aligned} \tag{A.10}$$

By comparing (A.7), we get the condition for $f(\rho, y, \phi)$ and $g(\rho, y, \phi)$ as follows;

$$\begin{aligned}
\frac{\partial f}{\partial \phi} &= -\frac{4q\rho^4 y}{(\rho^2 + y^2)^3}, \\
\frac{\partial g}{\partial \phi} &= \frac{4q\rho^3 y^2}{(\rho^2 + y^2)^3}, \\
\frac{\partial f}{\partial \rho} - \frac{\partial g}{\partial y} &= 0.
\end{aligned} \tag{A.11}$$

By integrating f and g with respect to ϕ , we get

$$f(\rho, y, \phi) = -\frac{4q\rho^4 y}{(\rho^2 + y^2)^3} (\phi + \phi_1)$$

$$g(\rho, y, \phi) = \frac{4q\rho^3 y^2}{(\rho^2 + y^2)^3}(\phi + \phi_2), \quad (\text{A.12})$$

but from the last condition of (A.11), we get $\phi_1 = \phi_2 = \phi_0$. Finally, 8-form potential can be written

$$\begin{aligned} C_{(8)} &= -\frac{4q\rho^4 y}{(\rho^2 + y^2)^3}(\phi + \phi_0)dt \wedge d\vec{x} \wedge d\Omega_3 \wedge dy \\ &\quad + \frac{4q\rho^3 y^2}{(\rho^2 + y^2)^3}(\phi + \phi_0)dt \wedge d\vec{x} \wedge d\Omega_3 \wedge d\rho. \end{aligned} \quad (\text{A.13})$$

If we fix location of D7 brane along ϕ direction at $\phi = \phi_*$, then (A.13) becomes total derivative i.e.

$$\begin{aligned} C_{(8)} &= -\frac{4q\rho^4 y}{(\rho^2 + y^2)^3}(\phi_* + \phi_0)dt \wedge d\vec{x} \wedge d\Omega_3 \wedge dy \\ &\quad + \frac{4q\rho^3 y^2}{(\rho^2 + y^2)^3}(\phi_* + \phi_0)dt \wedge d\vec{x} \wedge d\Omega_3 \wedge d\rho \\ &= (\phi_* + \phi_0) d \left[\frac{q\rho^4}{(\rho^2 + y^2)^2} dt \wedge d\vec{x} \wedge d\Omega_3 \right]. \end{aligned} \quad (\text{A.14})$$

so that $C_{(8)}$ is a pure gauge whose field strength is zero. Furthermore we can always choose $\phi_0 = -\phi_* + 2\pi$, then the Chen-Simons term in (3.3) becomes

$$\begin{aligned} S_{CS} &= \mu_7 \int d^8\sigma (2\pi) d \left[\frac{q\rho^4}{(\rho^2 + y^2)^2} dt \wedge d\vec{x} \wedge d\Omega_3 \right] \\ &= (2\pi)\mu_7 V_4 \Omega_3 \frac{q\rho^4}{(\rho^2 + y^2)^2} \Big|_{\rho=\infty} \\ &= q(2\pi)\mu_7 V_4 \Omega_3 \\ &= \frac{1}{2} N_{D(-1)}. \end{aligned} \quad (\text{A.15})$$

It is nothing but the half of D-instanton number calculated in [6]. This is completely satisfactory since D7 brane world volume can captures the flux of the upper hemi-sphere. Since the Chern-Simons action is locally a total derivative term, it does not contribute to the equation of motion.

B. Hamiltonian density of baryon vertex

We start from the action for D5 brane with Chern-Simons term (4.7),

$$\begin{aligned} S_{D5} &= S_{DBI} + S_{CS} \\ &= -\mu_5 \int e^{-\Phi} \sqrt{-\det(g + 2\pi\alpha' F)} + \mu_5 \int A_{(1)} \wedge G_{(5)} \\ &= \tau_5 \int dt d\theta \sin^4 \theta \left[-\sqrt{e^{\Phi} \frac{\omega^2}{\omega_+} (\xi^2 + \xi'^2) - \tilde{F}^2 + 4\tilde{A}_t} \right] \end{aligned}$$

$$= \int dt d\theta \mathcal{L}_{D5}, \quad (\text{B.1})$$

where

$$\tau_5 = \mu_5 \Omega_4 R^4 r_T, \quad \tilde{F} = 2\pi\alpha' F_{t\theta}, \quad \tilde{A}_t = 2\pi\alpha' A_t. \quad (\text{B.2})$$

We denote \mathcal{L}_{D5} to Lagrangian density. The displacement can be obtained by derivative of Lagrangian density with respect to A'_t ,

$$\begin{aligned} D(\theta) &\equiv -\frac{\partial \mathcal{L}_{D5}}{\partial A'_t} \\ &= -2\pi\alpha' \tau_5 \frac{\sin^4 \theta \tilde{F}}{\sqrt{e^{\Phi} \frac{\omega_-^2}{\omega_+} (\xi^2 + \xi'^2) - \tilde{F}^2}}. \end{aligned} \quad (\text{B.3})$$

Then the equation of motion for gauge field can be written as

$$\partial_\theta \hat{D}(\theta) = -4 \sin^4 \theta, \quad (\text{B.4})$$

where $\hat{D}(\theta) \equiv \frac{D(\theta)}{2\pi\alpha'\tau_5}$. This equation plays a constraint in the action, then the action of D5 brane becomes,

$$\begin{aligned} S_{D5} &= S_{DBI} + \tau_5 \int dt d\theta 4 \sin^4 \theta \tilde{A}_t \\ &= S_{DBI} - \tau_5 \int dt d\theta (\partial_\theta \hat{D}(\theta)) \tilde{A}_t \\ &= S_{DBI} - \tau_5 \int dt d\theta \hat{D} \tilde{F}, \end{aligned} \quad (\text{B.5})$$

where we take integration by part in last procedure. This is nothing but the Legendre transformation of DBI action of D5 brane. After substituting (B.3) in the the action, we define 'Hamiltonian density'(4.9) as follows

$$\begin{aligned} S_{D5} &= -\tau_5 \int dt d\theta \sqrt{\frac{e^{\Phi} \omega_-^2}{2 \omega_+} (\xi'^2 + \xi^2)} \sqrt{\hat{D}(\theta)^2 + \sin^8 \theta} \\ &\equiv - \int dt d\theta \mathcal{H}_{D5}. \end{aligned} \quad (\text{B.6})$$

The definition of Hamiltonian density is consistent with one of probe D7 brane and integration of this with on-shell solution gives free energy of D5 brane. Next, by integrating (B.4), we get

$$\hat{D}(\theta) = \frac{3}{2}(\nu\pi - \theta) + \frac{3}{2} \sin \theta \cos \theta + \sin^3 \theta \cos \theta, \quad (\text{B.7})$$

where the integration constant ν determines the number of fundamental strings on each pole, i. e. νN_c strings are attached to the south pole and $(1 - \nu)N_c$ strings to north pole of D5 brane. Here, we assume that all the fundamental strings are attached on the north pole, we set $\nu = 0$.

C. Force balance condition

In this section, we derive force balance condition (4.11). In our mode, the end points of fundamental strings play role of source of $U(1)$ gauge field. Due to the tension of fundamental string, there can exist cusps on probe brane world volume. By calculating force at the cusp of each brane, we can estimate the behavior of probe branes.

The force at the cusp can be obtained by taking small variation of 'on-shell' free energy with respect to U_c

$$F_c = \frac{\delta \mathcal{F}_{\text{on-shell}}}{\delta U_c}, \quad (\text{C.1})$$

where U_c is position of cusp and the free energy is integration of Hamiltonian density of probe brane

$$\mathcal{F} = \int d\rho \mathcal{H}_{\text{on-shell}}. \quad (\text{C.2})$$

The Hamiltonian density is a function of U and U' , we can write the variation as follows;

$$\begin{aligned} \delta \mathcal{H}_{\text{on-shell}} &= \delta \mathcal{H}(U, U'; \rho)_{\text{on-shell}} \\ &= \frac{\partial \mathcal{H}_{\text{on-shell}}}{\partial U} \delta U + \frac{\partial \mathcal{H}_{\text{on-shell}}}{\partial U'} \delta U' \\ &= \frac{\partial \mathcal{H}_{\text{on-shell}}}{\partial U} \delta U + \frac{d}{d\rho} \left[\frac{\partial \mathcal{H}_{\text{on-shell}}}{\partial U'} \delta U \right] - \frac{d}{d\rho} \left(\frac{\partial \mathcal{H}_{\text{on-shell}}}{\partial U'} \right) \delta U \\ &= \frac{d}{d\rho} \left[\frac{\partial \mathcal{H}_{\text{on-shell}}}{\partial U'} \delta U \right] + \left[\frac{\partial \mathcal{H}_{\text{on-shell}}}{\partial U} - \frac{d}{d\rho} \left(\frac{\partial \mathcal{H}_{\text{on-shell}}}{\partial U'} \right) \right] \delta U \\ &= \frac{d}{d\rho} \left[\frac{\partial \mathcal{H}_{\text{on-shell}}}{\partial U'} \delta U \right]. \end{aligned} \quad (\text{C.3})$$

Finally, the force at the cusp is

$$\begin{aligned} F_c &= \int d\rho \frac{\delta \mathcal{H}_{\text{on-shell}}}{\delta U_c} \\ &= \int d\rho \frac{d}{d\rho} \left[\frac{\partial \mathcal{H}_{\text{on-shell}}}{\partial U'} \frac{\delta U}{\delta U_c} \right] \\ &= \frac{\partial \mathcal{H}_{\text{on-shell}}}{\partial U'} \Big|_{U=U_c}. \end{aligned} \quad (\text{C.4})$$

The force at the cusp of single $D5$ brane can be calculated from (C.4),

$$F_{D5} = N_c T_{F1} \sqrt{\frac{e^\Phi \omega_-^2}{2 \omega_+} \frac{\xi'}{\sqrt{\xi^2 + \xi'^2}}} \Big|_{\xi=\xi_c}, \quad (\text{C.5})$$

where T_{F1} is tension of fundamental string $1/2\pi\alpha'$ and ξ_c is position of cusp of $D5$ brane. With a same manner, we can get force at the cusp of probe $D7$ brane,

$$F_{D7} = T_{F1} \sqrt{\frac{e^\Phi \omega_-^2}{2 \omega_+} \frac{Q\dot{y}}{\sqrt{1 + \dot{y}^2}}} \Big|_{y=y_c}, \quad (\text{C.6})$$

where y_c is position of $D7$ brane at the cusp($\rho = 0$) and Q is total number of $U(1)$ source. The force at the cusp of $D5$ and $D7$ is always smaller than the force of fundamental strings. Then strings pull each brane until the length of string becomes zero and force between two branes is balanced. We can get condition of slope of $D7$ brane from the force balance condition.

$$\begin{aligned}
0 &= F_{D7}(Q) + N_B F_{D5} \\
&= F_{D7}(Q) + \frac{Q}{N_c} F_{D5} \\
&\rightarrow \\
y_c &= \frac{\xi'_c}{\xi_c}. \tag{C.7}
\end{aligned}$$

References

- [1] E. Witten, *Adv. Theor. Math. Phys.* **2**, 505 (1998) [arXiv:hep-th/9803131].
- [2] E. Witten, *JHEP* **9807**, 006 (1998) [arXiv:hep-th/9805112].
- [3] C. G. . Callan, A. Guijosa, K. G. Savvidy and O. Tafjord, *Nucl. Phys. B* **555**, 183 (1999) [arXiv:hep-th/9902197].
- [4] Y. Seo and S. J. Sin, *JHEP* **0804**, 010 (2008) [arXiv:0802.0568 [hep-th]].
- [5] T. Schafer and E. V. Shuryak, *Rev. Mod. Phys.* **70**, 323 (1998) [hep-ph/9610451].
- [6] H. Liu and A. A. Tseytlin, *Nucl. Phys. B* **553**, 231 (1999) [arXiv:hep-th/9903091].
- [7] S. S. Gubser, arXiv:hep-th/9902155.
- [8] Y. Kim, B. H. Lee, C. Park and S. J. Sin, *Phys. Rev. D* **80**, 105016 (2009) [arXiv:0808.1143 [hep-th]].
- [9] K. Ghoroku, T. Sakaguchi, N. Uekusa and M. Yahiro, *Phys. Rev. D* **71**, 106002 (2005) [arXiv:hep-th/0502088].
- [10] K. Ghoroku and M. Ishihara, *Phys. Rev. D* **77**, 086003 (2008) [arXiv:0801.4216 [hep-th]].
- [11] S. J. Sin and Y. Zhou, *JHEP* **0905**, 044 (2009) [arXiv:0904.4249 [hep-th]].
- [12] K. Y. Kim, S. J. Sin and I. Zahed, “Dense hadronic matter in holographic QCD,” [arXiv:hep-th/0608046].
- [13] N. Horigome and Y. Tanii, *JHEP* **0701**, 072 (2007) [arXiv:hep-th/0608198].
- [14] S. Nakamura, Y. Seo, S. J. Sin and K. P. Yogendran, *J. Korean Phys. Soc.* **52**, 1734 (2008) [arXiv:hep-th/0611021];
S. Nakamura, Y. Seo, S. J. Sin and K. P. Yogendran, *Prog. Theor. Phys.* **120**, 51 (2008) [arXiv:0708.2818 [hep-th]].
- [15] S. Kobayashi, D. Mateos, S. Matsuura, R. C. Myers and R. M. Thomson, *JHEP* **0702**, 016 (2007) [arXiv:hep-th/0611099].
D. Mateos, S. Matsuura, R. C. Myers and R. M. Thomson, *JHEP* **0711**, 085 (2007) [arXiv:0709.1225 [hep-th]].
- [16] G. W. Gibbons, M. B. Green and M. J. Perry, *Phys. Lett. B* **370**, 37 (1996) [arXiv:hep-th/9511080].
- [17] A. Kehagias and K. Sfetsos, *Phys. Lett. B* **456**, 22 (1999) [arXiv:hep-th/9903109].
- [18] K. Ghoroku and M. Yahiro, *Phys. Lett. B* **604**, 235 (2004) [arXiv:hep-th/0408040].
- [19] M. Kruczenski, D. Mateos, R. C. Myers and D. J. Winters, *JHEP* **0307**, 049 (2003) [arXiv:hep-th/0304032].
- [20] J. Babington, J. Erdmenger, N. J. Evans, Z. Guralnik, I. Kirsch, *Phys. Rev.* **D69**, 066007 (2004). [hep-th/0306018].
- [21] M. Kruczenski, D. Mateos, R. C. Myers and D. J. Winters, *JHEP* **0405**, 041 (2004) [arXiv:hep-th/0311270].
- [22] J. Erdmenger, A. Gorsky, P. N. Kopnin, A. Krikun and A. V. Zayakin, *JHEP* **1103**, 044 (2011) [arXiv:1101.1586 [hep-th]].

- [23] M. A. Shifman, A. I. Vainshtein and V. I. Zakharov, Nucl. Phys. B **147**, 385 (1979).
- [24] D. Mateos, R. C. Myers and R. M. Thomson, Phys. Rev. Lett. **97**, 091601 (2006) [arXiv:hep-th/0605046].
D. Mateos, R. C. Myers and R. M. Thomson, JHEP **0705** (2007) 067 [arXiv:hep-th/0701132].
- [25] N. Evans, A. Gebauer, K. Y. Kim and M. Magou, JHEP **1003** (2010) 132 [arXiv:1002.1885 [hep-th]].
- [26] O. Bergman, G. Lifschytz and M. Lippert, “Holographic Nuclear Physics,” [arXiv:0708.0326].
- [27] O. Aharony, J. Sonnenschein and S. Yankielowicz, Annals Phys. **322**, 1420 (2007) [arXiv:hep-th/0604161].
- [28] M. Bianchi, M. B. Green, S. Kovacs and G. Rossi, JHEP **9808**, 013 (1998) [hep-th/9807033].
- [29] N. Dorey, T. J. Hollowood, V. V. Khoze, M. P. Mattis and S. Vandoren, Nucl. Phys. B **552**, 88 (1999) [hep-th/9901128].